

CONFIDENTIAL

Copy

NASA TM X-154

NASA TM X -154



# TECHNICAL MEMORANDUM

## X-154

PERFORMANCE OF A MACH NUMBER 3.0 DESIGN AXISYMMETRIC  
DOUBLE-CONE EXTERNAL-COMPRESSION INLET IN  
THE MACH NUMBER RANGE 1.97 TO 0.79

By Owen H. Davis and Glenn A. Mitchell

Lewis Research Center  
Cleveland, Ohio

DECLASSIFIED 8-9-63

Authority: NASA Memo to Holders of  
NASA Classified Material,  
Dtd. 8-9-63 Ref. BZC/REF: pas

CLASSIFIED DOCUMENT - TITLE UNCLASSIFIED

This material contains information affecting the national defense of the United States within the meaning of the espionage laws, Title 18, U.S.C., Secs. 793 and 794, the transmission or revelation of which in any manner to an unauthorized person is prohibited by law.

NATIONAL AERONAUTICS AND SPACE ADMINISTRATION  
WASHINGTON

April 1960

CONFIDENTIAL

CONFIDENTIAL

## NATIONAL AERONAUTICS AND SPACE ADMINISTRATION

## TECHNICAL MEMORANDUM X-154

## PERFORMANCE OF A MACH NUMBER 3.0 DESIGN AXISYMMETRIC

## DOUBLE-CONE EXTERNAL-COMPRESSION INLET IN THE

## MACH NUMBER RANGE 1.97 TO 0.79\*

By Owen H. Davis and Glenn A. Mitchell

## SUMMARY

The off-design performance of a double-cone external-compression inlet was investigated at Mach numbers from 1.97 to 0.79 in order to extend data previously reported on a geometrically similar model from the design Mach number of 3.0 to 1.48. Briefly examined also was the effect of cowl-lip projected area on the relative balance between additive and cowl drags. In addition, the study simulated the variable-geometry feature of a translating first cone with the intent of using separated flow to form effectively a single-cone inlet. Oblique-shock rather than normal-shock spillage might thus be obtained at off-design Mach numbers as a drag-reducing technique.

In the basic off-design study, maximum subcritical total-pressure recoveries increased from about 0.92 to 0.99 between Mach numbers 1.97 and 0.79; values at critical flow were only slightly less. The greatest supercritical mass-flow spillage, about 62 percent, occurred in the transonic region. Total drag coefficient peaked in the vicinity of Mach number 1.4 and fell off rapidly (0.43 to 0.10) between Mach numbers 1.28 and 0.79.

The increase in additive drag incurred by a change in cowl-lip projected area from 20 to 10 percent of the maximum frontal area was offset by a reduction in cowl drag such that the total drags of the two configurations were essentially the same.

Use of extended first cones showed that it was possible in this situation for separated flow to form part of the external-compression surface. This technique reduced drags considerably, especially at the higher Mach numbers, but at the expense of large losses in total-pressure recovery.

---

\*Title, Unclassified.

CONFIDENTIAL

## INTRODUCTION

Reported in references 1 to 3 is the performance of a double-cone axisymmetric inlet having a projected cowl-lip area equal to 20 percent of the frontal area, and designed at Mach number 3.0 for all-external compression. The data therein, which include the speed range of Mach number 3.01 to 1.48, show that one of the off-design operational problems is the drag rise that occurs with flow detachment from the second cone. For the present study a geometrically similar model was used to extend the data to transonic and subsonic Mach numbers with emphasis given to experimentally defining the drag characteristics in the cone shock-detachment speed range.

As an adjunct to the study of inlet performance, a brief examination was made of the effect of cowl projected area on the relative balance or "trade-off" between additive and cowl pressure drags. For this purpose the cowl of 20-percent projected area was alternately replaced with cowls giving the same throat area but having zero and 10-percent projected frontal area. Also studied were configurations that simulated an extendible first cone with the second cone stationary. This variable feature could conceivably be used in reducing the drag associated with a detached second-cone shock, provided separated flow bridged between the cones to produce effectively a single-cone inlet.

The tests were conducted in the NASA Lewis 8- by 6-foot tunnel at  $0^\circ$  angle of attack at free-stream Mach numbers of 1.97, 1.48, 1.28, 1.00, and 0.79.

## SYMBOLS

$A$	area, sq ft
$A_f$	flow area at the model inlet
$A_{in}$	inlet capture area (20% cowl, 0.713 sq ft; 10% cowl, 0.787 sq ft; 0% cowl, 0.886 sq ft)
$A_{max}$	maximum cross-sectional area of body, 0.886 sq ft
$C_D$	drag coefficient, $D/q_0 A_{max}$
$C_{D,a}$	additive-drag coefficient
$C_{D,c}$	cowl drag coefficient
$C_{D,f}$	friction-drag coefficient

CONFIDENTIAL

- $C_{D,t}$  total drag coefficient,  $C_{D,c} + C_{D,f} + C_{D,a}$
- $C_p$  pressure coefficient  $(p - p_0)/q_0$
- $D$  drag
- $M$  Mach number
- $m_3/m_0$  mass-flow ratio,  $\rho_3 V_3 A_3 / \rho_0 V_0 A_{in}$
- $P$  total pressure, lb/sq ft
- $\frac{\Delta P_3}{P_0}$  diffuser-exit flow-distortion parameter,  $\frac{P_{3,max} - P_{3,min}}{\bar{P}_3}$
- $p$  static pressure, lb/sq ft
- $q$  dynamic pressure, lb/sq ft
- $r$  spike radius
- $V$  velocity, ft/sec
- $w$  weight flow, lb/sec
- $\frac{w\sqrt{\theta}}{\delta A_3}$  corrected weight flow per unit area, (lb/sec)/sq ft
- $x$  distance along axis of symmetry
- $\delta$  ratio of total pressure to NASA standard sea-level pressure of 2116.2 lb/sq ft
- $\theta$  ratio of total temperature to NASA standard sea-level temperature of 518.7° R
- $\theta_1$  spike-position parameter (angle between axis of symmetry and line from spike tip to cowl leading edge), deg
- $\rho$  density of air, slugs/cu ft

Subscripts:

- max maximum
- min minimum

CONFIDENTIAL

th            throat  
 0            free stream  
 3            diffuser exit

Superscript:

—            average

### APPARATUS AND PROCEDURE

Figure 1(a) presents a schematic drawing of the model showing the inlet mounted on its cylindrical sting-supported afterbody. Because of the length of the afterbody, an external shroud, supported independently of the metric portion of the model, was used as a shield against tunnel-wall shock reflections. The basic inlet of the study had a cowl projected area 20 percent of the maximum frontal area and was geometrically identical (to the throat station) to the inlet reported in references 1 and 2. The cone half-angles of the double-cone spike were  $20^\circ$  and  $35^\circ$ . The inlet was designed for Mach number 3.0 with the shocks from the double cone coalescing at the cowl lip at that Mach number for the spike-position parameter  $\theta_7$  of  $29.5^\circ$ . The second-cone shock could be maintained at the cowl lip by increasing  $\theta_7$  to  $31.3^\circ$  with a Mach number decrease to 2.07. Below this Mach number the second-cone shock theoretically detaches and hence was so detached at the Mach numbers (1.97 to 0.79) of the present study.

In addition to the basic cowl of 20-percent projected area, two cowls having zero and 10-percent projected area were employed in the program. (Cowl contours are given in fig. 1(b).) The latter cowls, using the same spike as the 20-percent cowl, were not intended to form practical inlets but were intended only to provide a systematic variation of cowl projected area for a brief study of the balance between additive and cowl pressure drags. Throat areas for the two cowls of smaller projected area were made equal (within manufacturing tolerances) to that of the 20-percent cowl at its design spike position of  $29.5^\circ$ .

As a secondary point of interest in the program, two extended-spike configurations shown in figure 1(c) were used to simulate a translating first cone. These configurations were tested with the 20-percent cowl and will be called the  $20^\circ$ - and  $13^\circ$ -extended spikes, referring to the angle between the model centerline and the line from the spike tip to the second-cone shoulder.

The distribution of flow area for all configurations and spike positions tested is shown in figure 2. As shown in the table with the

figure, all configurations have internal contraction except the 20-percent cowl at  $\theta_7$  of  $29.5^\circ$ . For this configuration, the subsonic diffuser angle, expressed in terms of an equivalent conical diffuser, is  $20.1^\circ$  for such a diffuser having the same area change in the first 3 inches of diffusion and is  $6.0^\circ$  for a conical diffuser having the same area change per unit hydraulic diameter (the same wetted area per unit area change).

The model was instrumented to obtain mass flow, compressor-face total-pressure recovery, external and internal cowl pressures, spike pressures, and throat total-pressure recovery (see fig. 1). An internal strain-gage balance measured axial forces.

Additive drag was obtained by two methods, a comparison of which is shown in figure 3. The first method used differences in inlet and free-stream momenta as determined by the inlet rake in conjunction with internal cowl and spike static pressures. In the second method, the additive drag was calculated by the difference between total external drag and cowl plus friction drag ( $C_{D,a} = C_{D,t} - C_{D,f} - C_{D,c}$ ). (The friction-drag coefficient was not measured; it was computed based on flat-plate turbulent flow and varied almost linearly from 0.024 to 0.018 for the Mach number range of 0.79 to 1.97.) The two techniques gave additive-drag values that generally were in good agreement. However, using the drag-difference method, slightly better results were obtained near critical mass flow, where the momenta-difference method proved sensitive to the flow distortions at the inlet throat. In the body of the report the additive drag presented is that computed by the drag-difference method.

Data were obtained with the model installed in the transonic test section of the NASA Lewis 8- by 6-foot wind tunnel with the model at zero angle of attack at Mach numbers of 0.79, 1.00, 1.28, 1.48, and 1.97.

## RESULTS AND DISCUSSION

### Performance of Inlet with 20-Percent Cowl

The variations with mass-flow ratio of total drag, cowl drag, total-pressure recovery, and flow distortion are presented in figure 4 for three spike positions. Figure 5 summarizes the effect of free-stream Mach number on the values of the drag coefficients, pressure recoveries, and mass-flow ratios at critical flow.

Except for the performance at Mach number 1.97, the stable mass-flow range was practically unlimited at the Mach numbers of this study. The mass-flow spillages at critical flow were greatest in the transonic region. As much as 62-percent mass flow was spilled at Mach number 1.00 for  $\theta_7 = 29.5^\circ$ , and slightly less for the more retracted spike positions.

Maximum or peak pressure recovery was independent of spike position at all Mach numbers except 1.97. The maximum values of pressure recovery increased from about 92 percent at Mach number 1.97 to about 99 percent at 0.79; values at critical flow were only slightly less.

Flow distortions were essentially independent of spike position. Values at critical flow were generally under 10 percent.

Previous data for this inlet showed almost a fourfold increase in critical total drag coefficient with a reduction in Mach number from the design value of 3.0 to a value of 1.48. The present data (fig. 5) show the drag coefficient to peak in the vicinity of Mach number 1.4, with a rapid decrease at Mach numbers below 1.28. For example, at  $\theta_l = 29.5^\circ$ , the total drag coefficient decreased from 0.43 to 0.10 between Mach numbers 1.28 and 0.79. This fall-off with decreasing Mach number results from the significant drop in both additive- and cowl-drag coefficients. At Mach numbers 1.00 and 0.79 the cowl drag was negative (producing thrust) even at critical flow; at the higher Mach numbers negative cowl drag was measured only at subcritical mass flows. With decreasing Mach numbers, it appeared that the cowl thrust increased while the additive drag decreased, but the data (fig. 5) are not sufficient to permit extrapolation to a subsonic Mach number at which the two forces would be in balance.

An engine-matching analysis for this inlet design is made in reference 4 for the Mach number range of 0.79 to 3.0 using the data of this report and those of references 1 to 3.

#### Effect of Cowl-Lip Projected Area

Figure 6 compares the subcritical additive- and cowl-drag coefficients of the 0-, 10- and 20-percent cowls for the spike extensions that provide identical throat areas. Critical values of the two drag coefficients and their sum are summarized in figure 7 as a function of free-stream Mach number.

At each Mach number the mass flows for all configurations in figure 6 are referenced to the same denominator, the mass flow based on the capture (lip) area of the 20-percent cowl. Thus, comparison of the actual mass flows of the configurations is facilitated. Except at Mach number 1.97, all configurations had essentially the same critical mass flow (which indicates nearly identical throat pressure recovery, since the throats were of the same size and choked).

At all Mach numbers including subsonic, additive drag at critical flow increased with decreasing cowl projected area and with spike retraction. The cowl drags at critical flow decreased appreciably in changing

E-151

from the 20- to the 10-percent cowl (producing thrust at all Mach numbers), and decreased slightly with spike retraction. For  $\theta_2 = 29.5^\circ$ , the decrease in cowl drag was able to balance or exceed the increase in additive drag, as shown by the sum of the two drags in figure 7. For this configuration (10-percent cowl), data were available only down to Mach number 1.28, but extrapolation indicates the same balance of additive drag with cowl thrust probably would persist at the lower Mach numbers as well. Subcritical inlet operation would probably favor the 20-percent cowl in a comparison of the total drags, because the 20-percent cowl showed a much larger reduction in cowl drag with decreasing mass flow than did the 10-percent cowl.

Cowl pressure distributions at critical flow are illustrated in figure 8 for both the 10- and 20-percent cowls.

### Cone Pressure Profiles

At the present time there exists no technique for predicting the additive drag of a double-cone inlet over its full range of flight Mach number and mass-flow ratio. Such a theory must predict the spike pressures as was done successfully for the single-cone inlet in reference 5. However, with the two-cone inlet this problem is much more involved. Here the normal (spillage) shock may impinge on either cone; in addition, the pressures resulting from shock detachment from either or both of the two cones must be handled by the analysis. Viscous effects also play an important part, primarily as they concern shock-induced flow detachment from the spike. The complicated nature of double-cone pressure distributions is illustrated by the data of the present study. Typical spike pressure coefficients for the 0-, 10-, and 20-percent-cowl configurations are shown in figure 9 for critical flow, and pressure coefficients for the 20-percent cowl for subcritical flows are shown in figure 10. Theoretical values of first-cone pressure coefficients are given in figure 10. The shocks theoretically detach below Mach numbers of 2.07 and 1.21 for the second and first cones, respectively. The second cone starts on the abscissa at a value of  $r^2/r_{\max}^2$  of 0.35.

The location, magnitude, and steepness of the pressure rise on the spike in a given case are related to one of the many possible flow fields in which the second-cone shock is either (1) essentially attached (fig. 10(c) at Mach number 1.97), or (2) is detached (fig. 9(a) at Mach number 1.48). Subcritically, the spillage shock may (a) stand on the second cone (fig. 10(c)) or (b) move ahead of this cone and merge with the detached second-cone shock (figs. 10(a) and (b)). In this last case, viscous effects may result in the pressure rise being felt out to the very tip of the first cone. Thus it may be impossible to predict even the initial values of the first-cone pressures at Mach numbers where the first-cone shock should be attached. Schlieren observation of the flow

was not possible in this study, but such photographs are shown in reference 1 for the 20-percent cowl at Mach numbers between 1.48 and 1.97.

As an incidental observation, pressures on the cone at critical flow were remarkably similar for different cowl sizes when the spike-projection angles  $\theta_1$  were the same. This is seen for example in the comparison of the 20- and 10-percent cowls at  $\theta_1 = 29.5^\circ$  (figs. 9(a) and (b)) and the 10- and 0-percent cowls at  $\theta_1 = 32.1^\circ$  (figs. 9(b) and (c)).

#### Extended First Cones

A secondary phase of this study involved configurations simulating an extendible first cone as a technique for circumventing the high spillage drag associated with a detached second-cone shock. Schlieren studies, as illustrated in figure 11, of spikes at Mach number 1.91 in a smaller tunnel showed that, effectively, a single-cone configuration could be derived from a two-cone spike with separated flow bridging the gap between the shoulder of the second cone and the shoulder of the extended first cone. In the present test, two cone extensions were studied using the 20-percent-cowl configuration with the second cone remaining in the Mach number 3.0 position.

The performances of these configurations as total-pressure recovery, distortion, total drag, and cowl drag are presented in figure 12 against mass-flow ratio. The performance of these inlets at critical flow conditions is compared with that of the normal double-cone 20-percent-cowl configuration in figure 13.

At critical flow, the extended-spike configurations decreased the additive drag and hence total drag over the entire Mach number range, the greatest reductions occurring at the higher Mach numbers. These drag savings were made despite the fact that the extended spikes spilled more mass flow than did the fixed-spike inlet. If the fixed-spike inlet were operated at the same mass flow as the extended spikes, the increased drag due to subcritical operation would make the drag reduction of the extended spikes even more pronounced (e.g., see the dashed drag curve of fig. 13 representing the drag of the fixed spike operating at the mass flow of the 20<sup>o</sup>-extended spike).

Total-pressure recoveries were considerably decreased with the extended spikes. A throat bleed system might improve pressure recoveries by removing low-energy separated flow that is apparently entering the inlets. It is also probable that the shock system itself is not efficient.

CONFIDENTIAL

The data indicate that it is possible to use separated flow to form part of an external-compression surface. However, the gains in drag and losses in pressure recovery would certainly have to be weighed in an engine-inlet matching analysis before judging the merit of an extendible first cone as a variable-geometry feature. The effects of angle of attack, not part of this study, would also have to be considered.

#### SUMMARY OF RESULTS

The performance of a double-cone external-compression Mach 3.0 design inlet was investigated in the Lewis 8- by 6-foot tunnel at Mach numbers from 1.97 to 0.79. The inlet cowl had a projected frontal area equal to 20 percent of the maximum frontal area. A comparison was made of the drag characteristics of this cowl and cowls having zero and 10-percent projected frontal area.

Also studied were two inlets that simulated translating first cones designed to reduce drag by oblique rather than bow-shock spillage. The following results were obtained:

1. The Mach 3.0 design inlet spilled as much as 62 percent of the mass flow in the transonic region. Maximum values of total-pressure recovery increased from about 0.92 to 0.99 between Mach numbers 1.97 and 0.79; values at critical flow were only slightly less. Total drag coefficient peaked in the vicinity of Mach 1.4 and fell off rapidly (0.43 to 0.10) between Mach numbers 1.28 and 0.79.

2. Essentially the same total drags were measured in changing from the 20-percent to the 10-percent cowls (with the same relative spike positions), since the increase in additive drag due to increased spillage was offset by the decrease in cowl drag.

3. Use of extended first cones showed that it was possible to use separated flow to form part of the external-compression surface. This technique reduced drags considerably, especially at the higher Mach numbers, but at the expense of large losses in total-pressure recovery.

Lewis Research Center

National Aeronautics and Space Administration  
Cleveland, Ohio, December 17, 1959

CONFIDENTIAL

CONFIDENTIAL

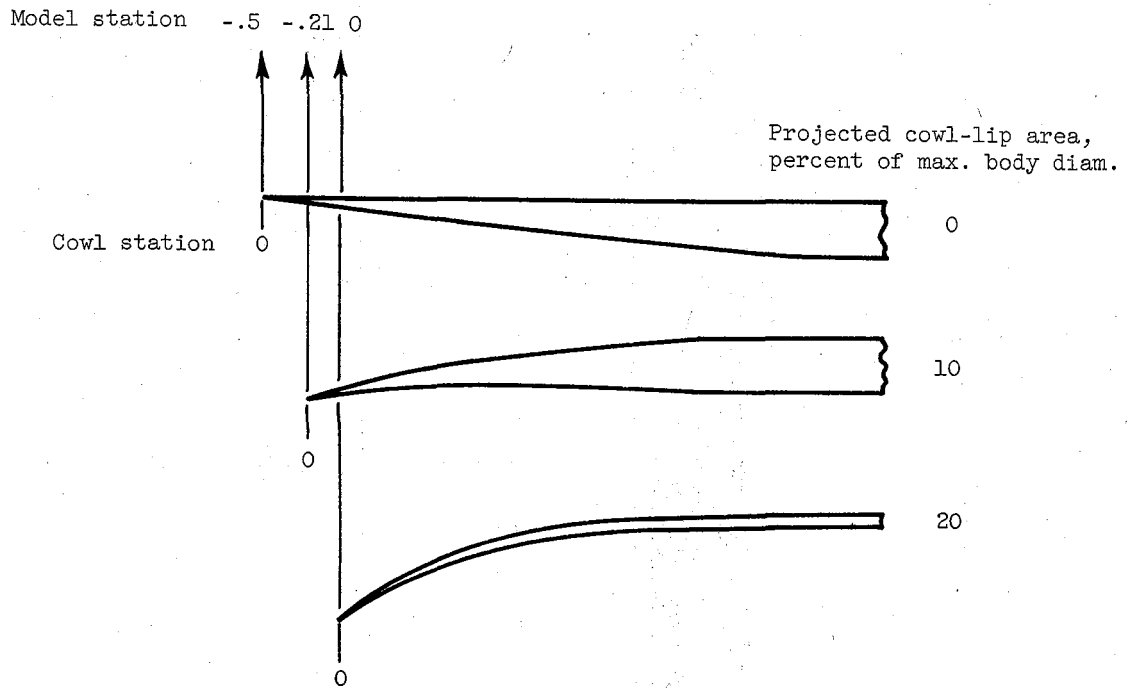
## REFERENCES

1. Allen, John L., and Mitchell, Glenn A.: Performance of a Mach Number 3.0 Design Axisymmetric Double-Cone External-Compression Inlet in Mach Number Range 2.07 to 1.48. NASA MEMO 12-22-58E, 1959.
2. Connors, James F., Lovell, J. Calvin, and Wise, George A.: Effects of Internal-Area Distribution, Spike Translation, and Throat Boundary-Layer Control on Performance of a Double-Cone Axisymmetric Inlet at Mach Numbers from 3.0 to 2.0. NACA RM E57F03, 1957.
3. Connors, James F., Wise, George A., and Lovell, J. Calvin: Investigation of Translating-Double-Cone Axisymmetric Inlets with Cowl Projected Areas 40 and 20 Percent of Maximum at Mach Numbers from 3.0 to 2.0. NACA RM E57C06, 1957.
4. Allen, John L., Davis, Owen H., and Mitchell, Glenn A.: Performance Summary and Analysis of a Mach 3.0 Design Axisymmetric All-External-Compression Double-Cone Inlet From Mach Number 3.0 to 0.8. NASA TM X-149, 1960.
5. Sibulkin, Merwin: Theoretical and Experimental Investigation of Additive Drag. NACA Rep. 1187, 1954. (Supersedes NACA RM E51B13.)

E-151

CONFIDENTIAL



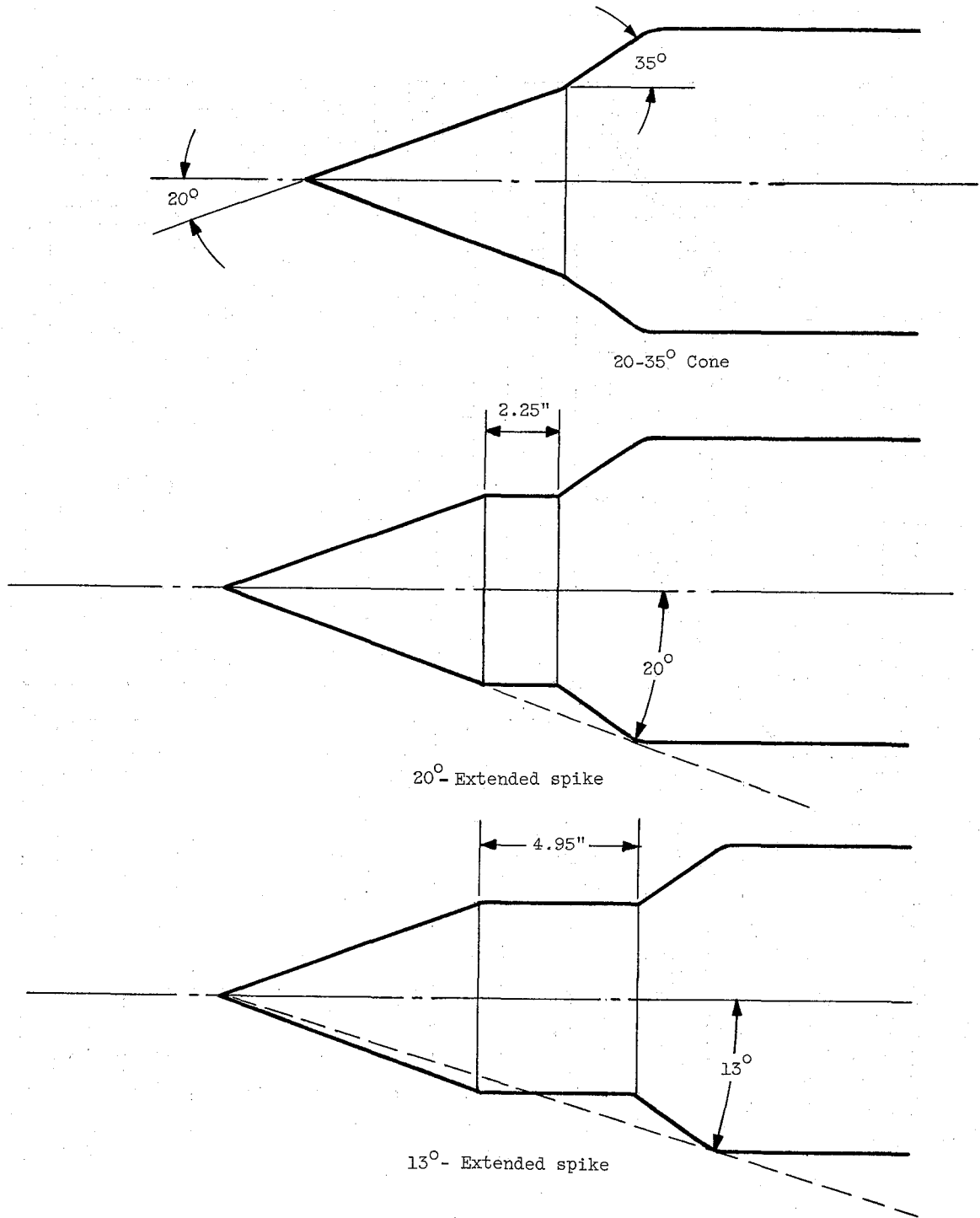


E-151

Sta- tion	Cowl					
	0%		10%		20%	
	Radii, in.					
	Ext.	Int.	Ext.	Int.	Ext.	Int.
0.00	6.36	6.36	6.01	6.00	5.72	5.71
.25	6.37	6.34	6.07	6.03	5.89	5.84
.50		6.31	6.13	6.06	6.03	5.96
.75		6.29	6.17	6.08	6.14	6.06
1.00		6.26	6.21	6.09	6.21	6.12
1.25		6.24	6.25	6.10	6.27	6.17
1.50		6.22	6.28	6.10	6.30	6.20
1.75		6.20	6.30	6.10	6.32	6.23
2.00		6.17	6.32	6.09	6.34	6.24
2.25		6.15	6.34	6.08	6.35	6.25
2.50		6.13	6.35	6.07	6.36	6.26
2.75		6.10	6.36	6.06	6.37	6.27
3.00		6.08	6.37	6.05		
3.25		6.06		6.04		
3.50		6.04				
3.75						
3.89						
4.00						6.28

(b) Cowl configurations.  
Figure 1. - Continued. Model details.

E-151



CD-6674

(c) Spike configurations.  
Figure 1. - Concluded. Model details.

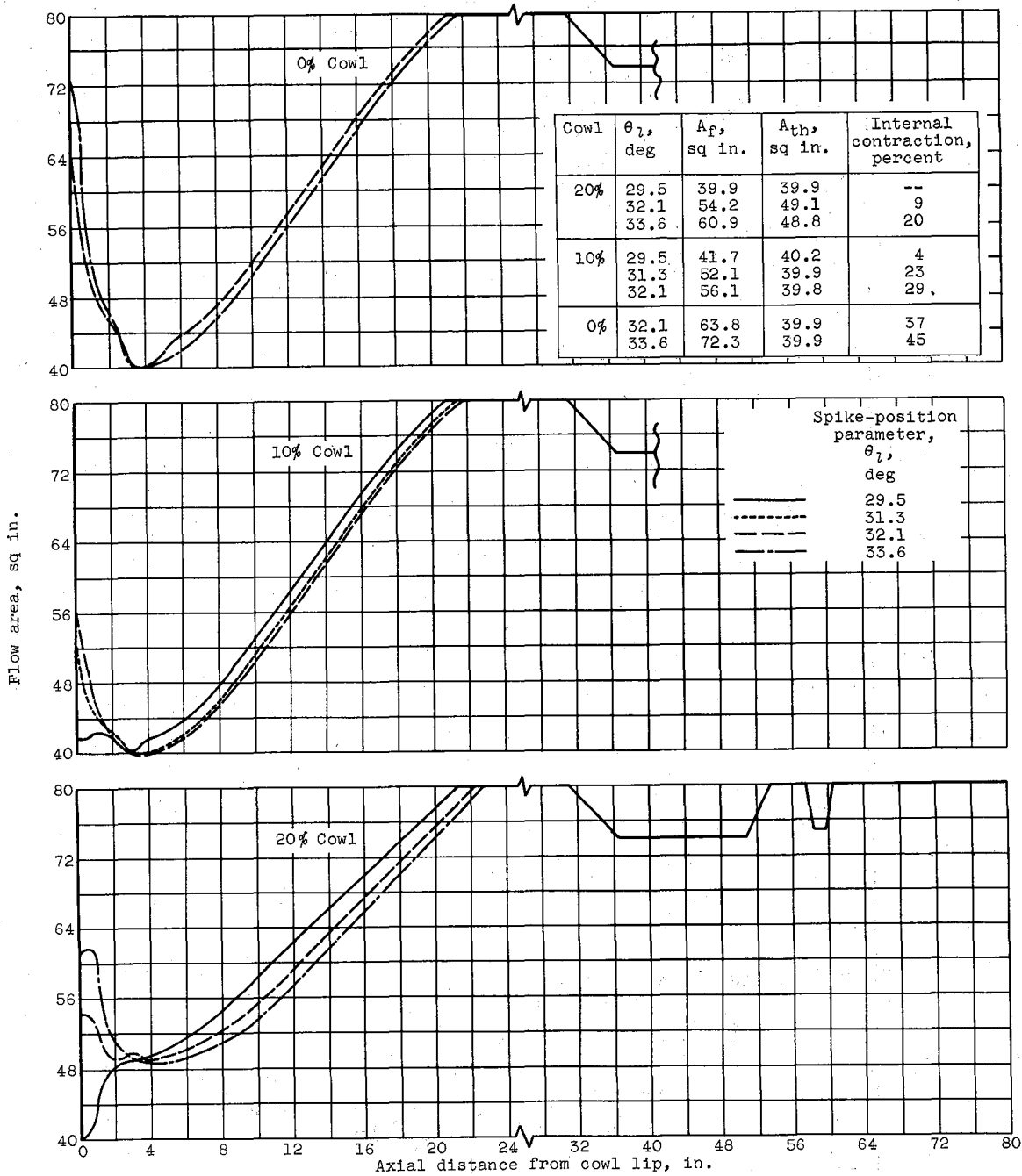


Figure 2. - Internal area distributions.

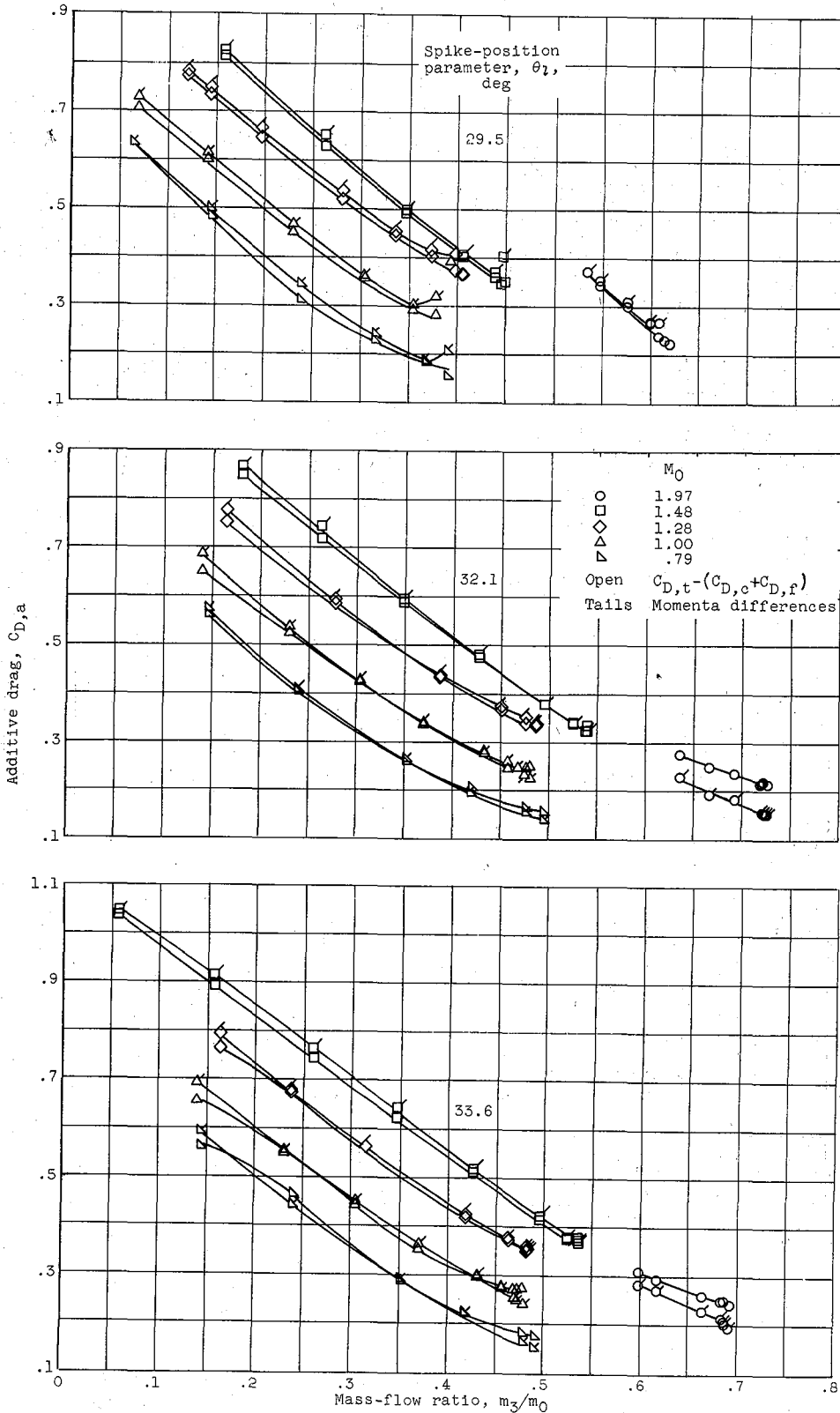
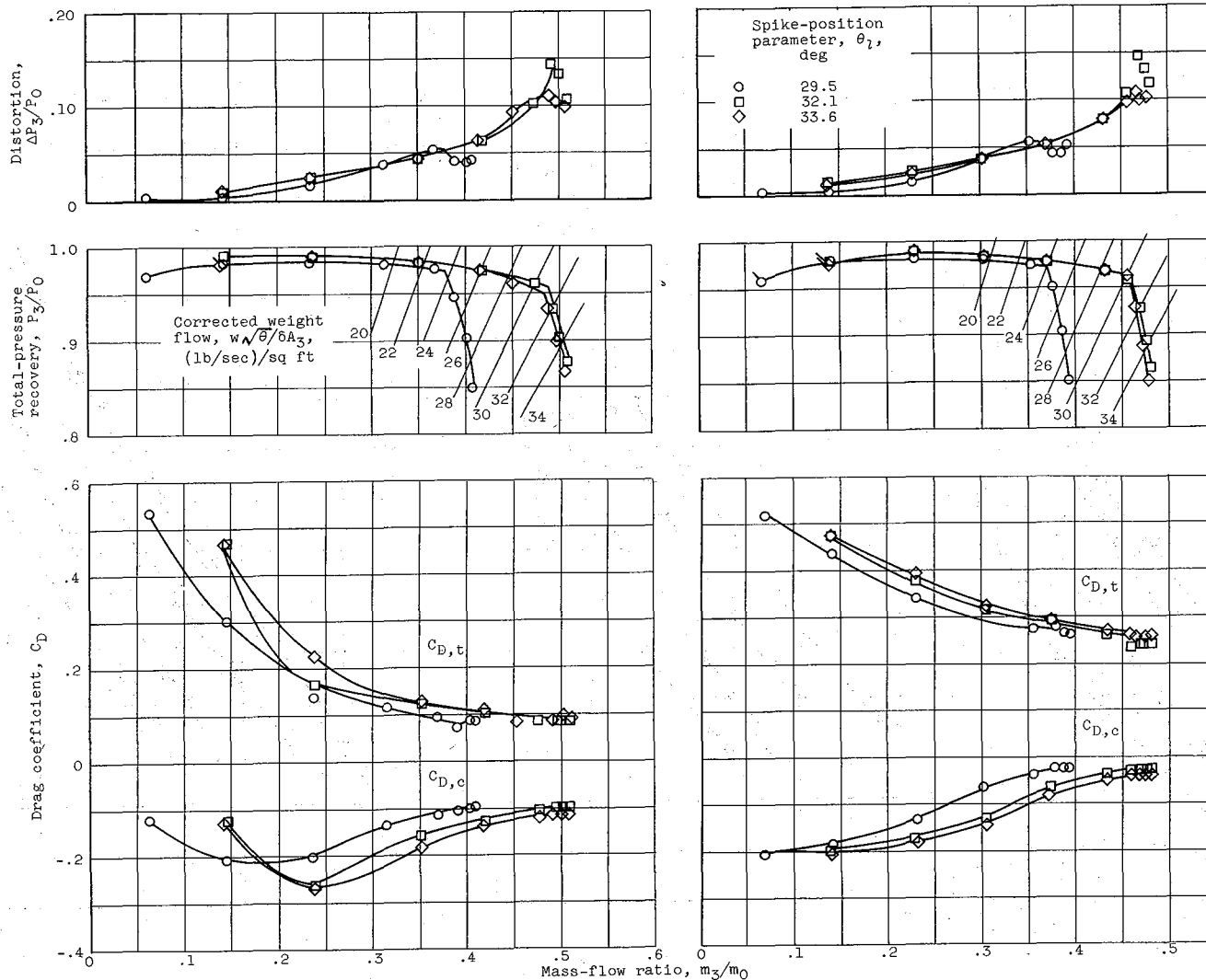


Figure 3. - Comparison of additive drags computed by two methods for 20-percent cowl.

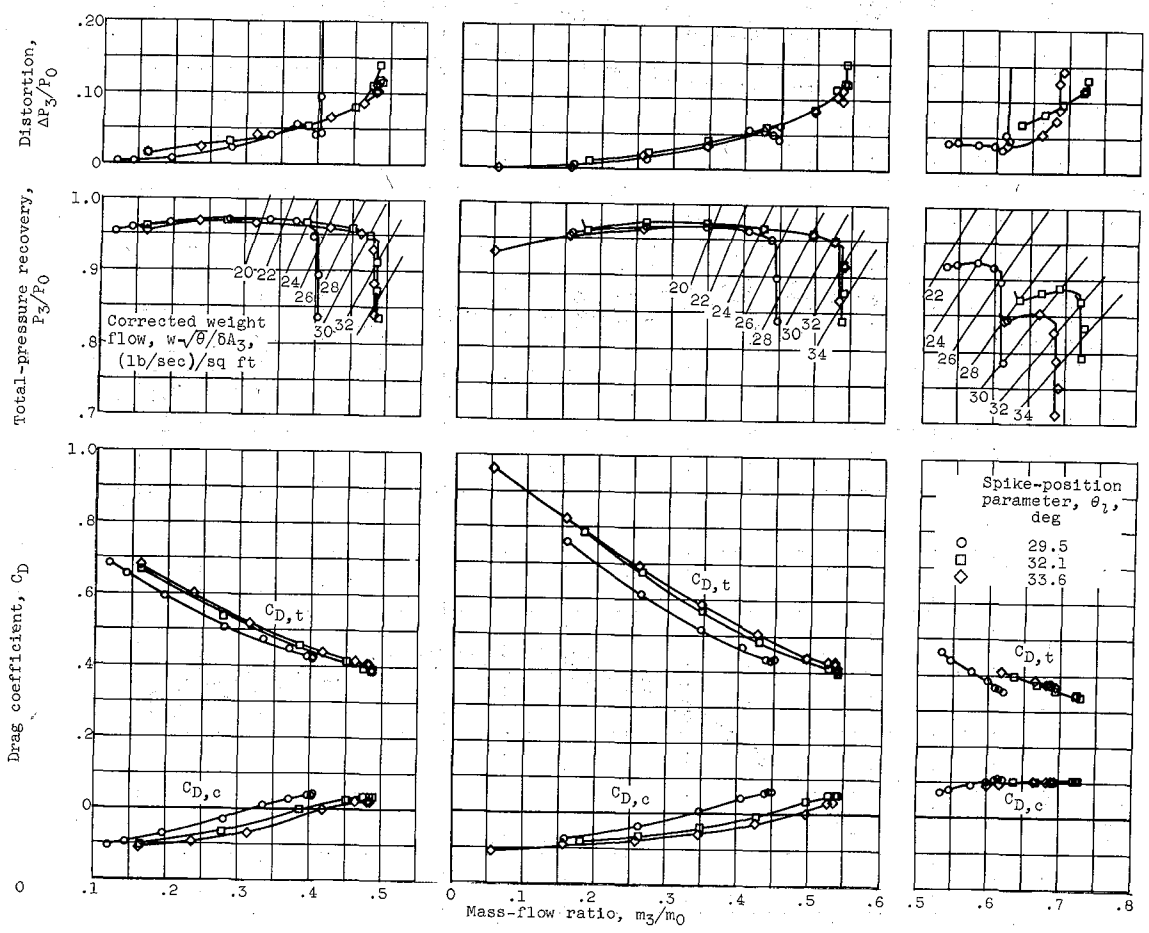
E-151



(a) Free-stream Mach number, 0.79.

(b) Free-stream Mach number, 1.00.

Figure 4. - Inlet performance characteristics for 20-percent cowl configuration.



(c) Free-stream Mach number, 1.28.

(d) Free-stream Mach number, 1.48.

(e) Free-stream Mach number, 1.97.

Figure 4. - Concluded. Inlet performance characteristics for 20-percent-cowl configuration.

CONFIDENTIAL

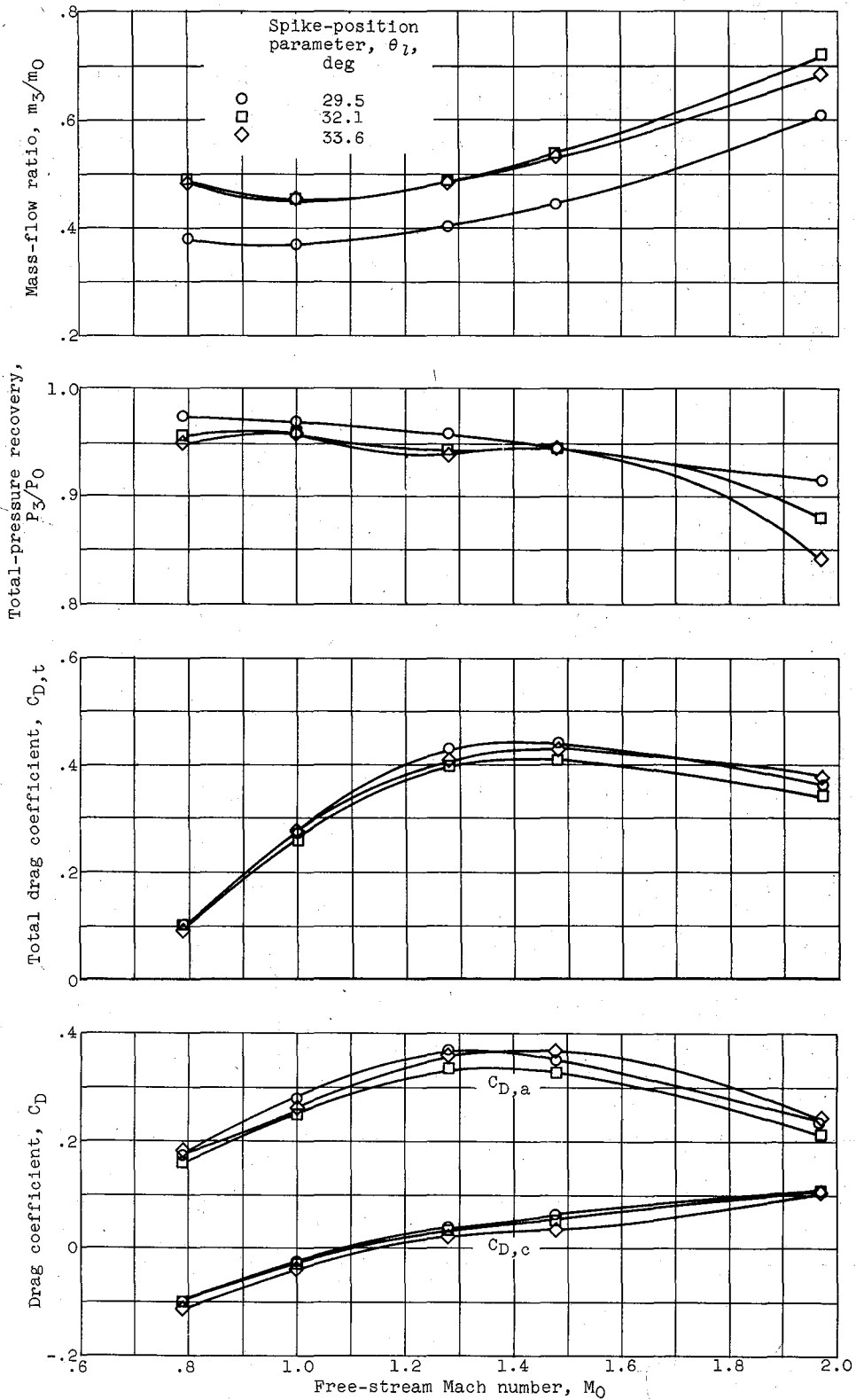
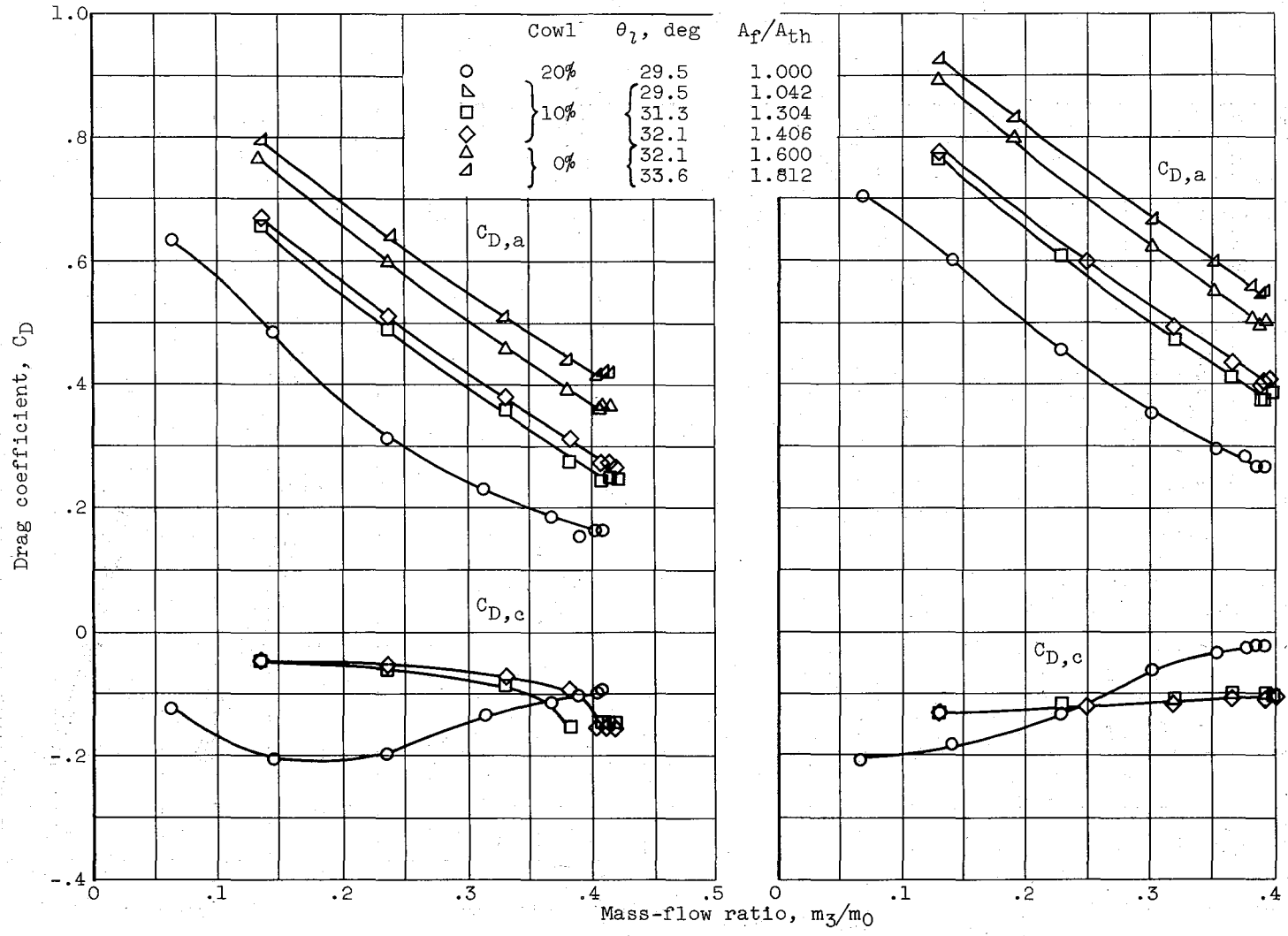


Figure 5. - 20-Percent-cowl performance at critical mass-flow ratio.

CONFIDENTIAL

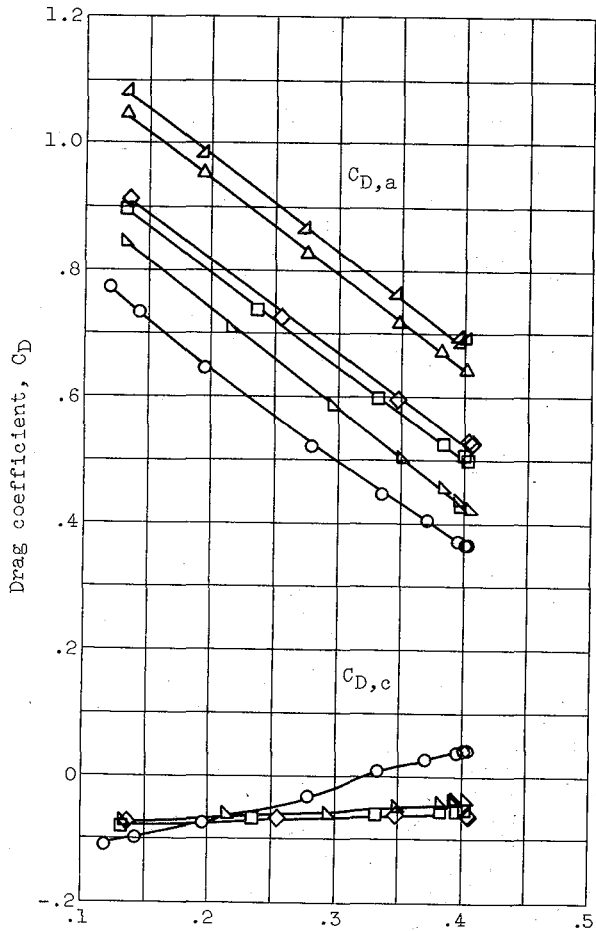
CONFIDENTIAL



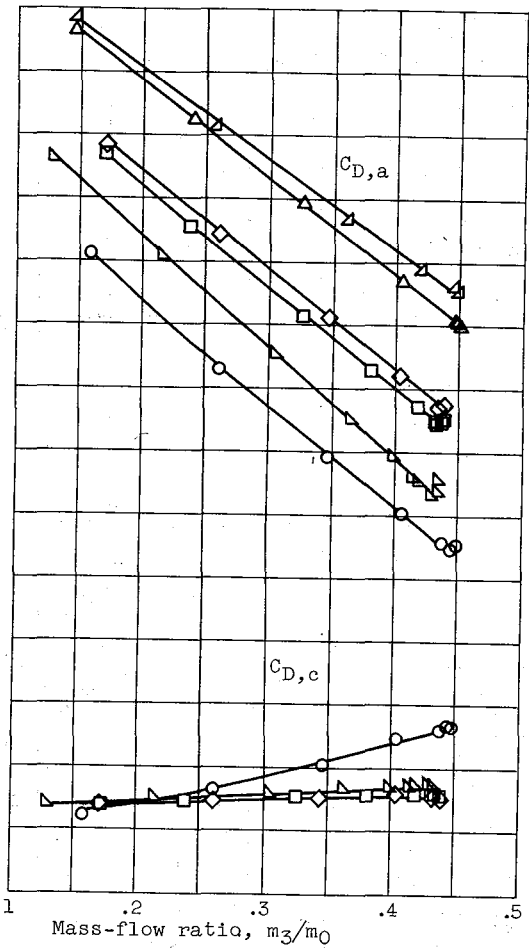
(a) Free-stream Mach number, 0.79. (b) Free-stream Mach number, 1.00.

Figure 6. - Comparison of additive and cowl drags for 0-, 10-, and 20-percent cowls.

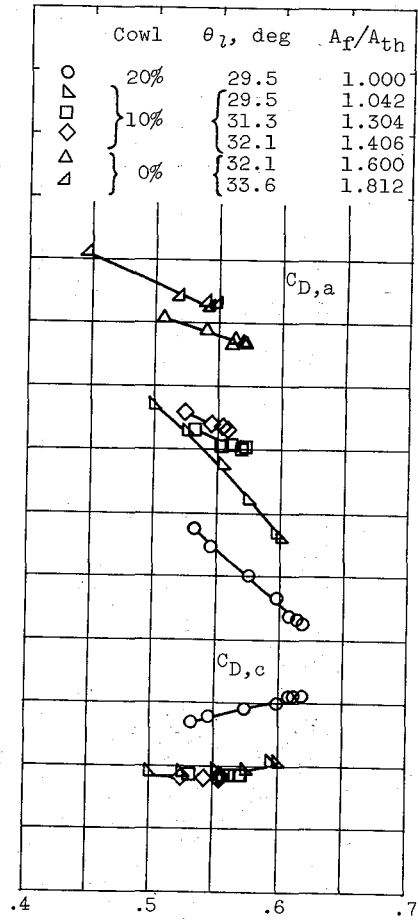
CONFIDENTIAL



(c) Free-stream Mach number, 1.28.

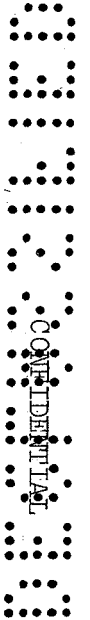


(d) Free-stream Mach number, 1.48.



(e) Free-stream Mach number, 1.97.

Figure 6. - Concluded. Comparison of additive and cowl drags for 0-, 10-, and 20-percent cowls.



CONFIDENTIAL

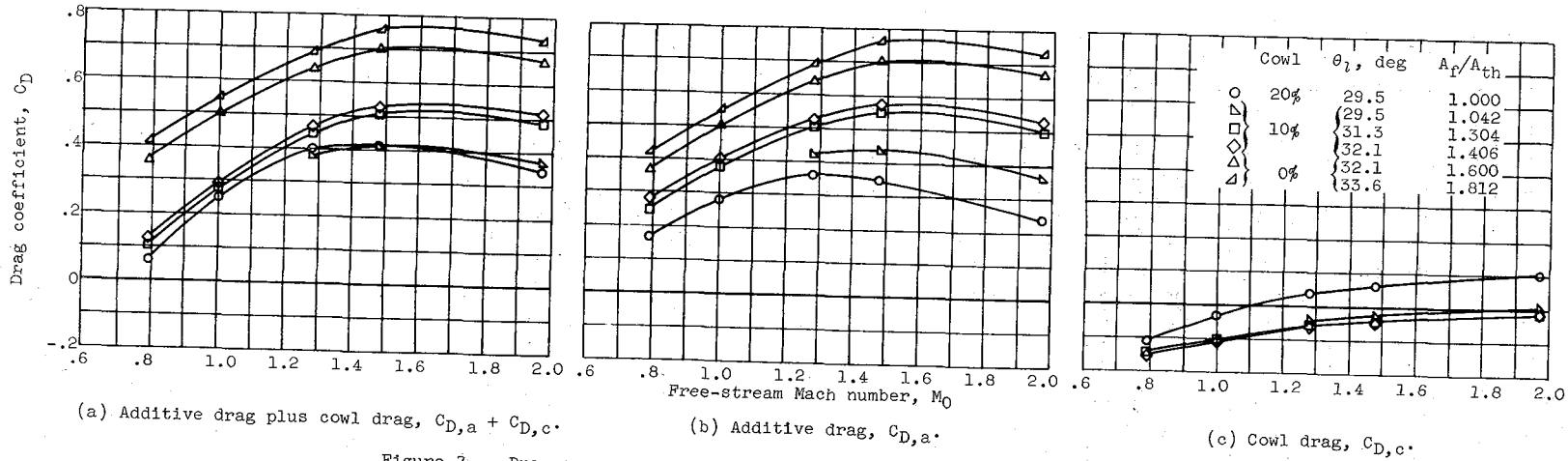


Figure 7. - Drag summary at critical inlet flow for 0-, 10-, and 20-percent cowls.

CONFIDENTIAL

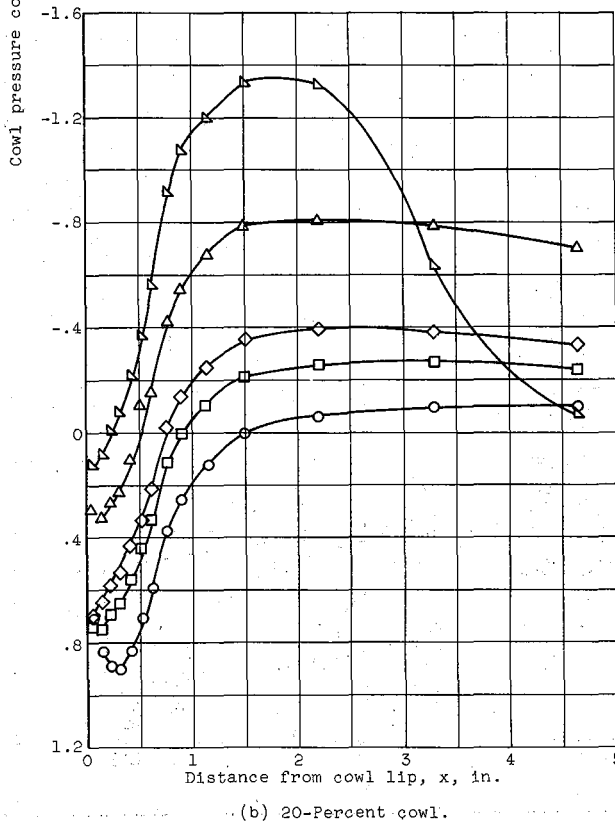
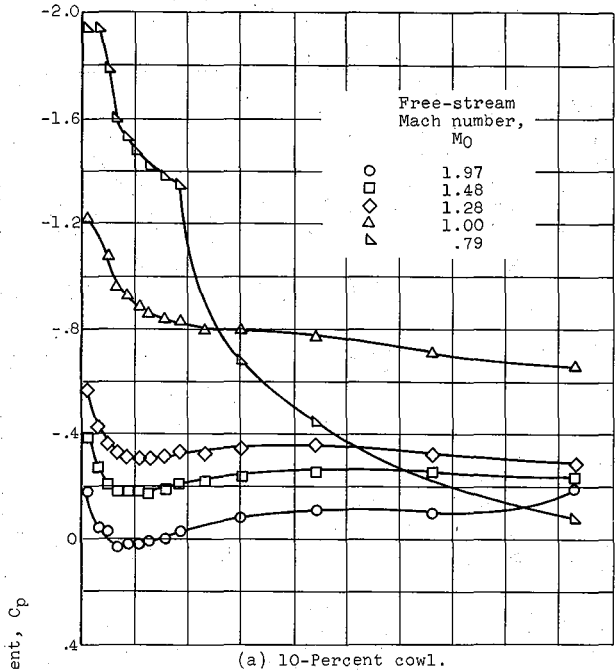
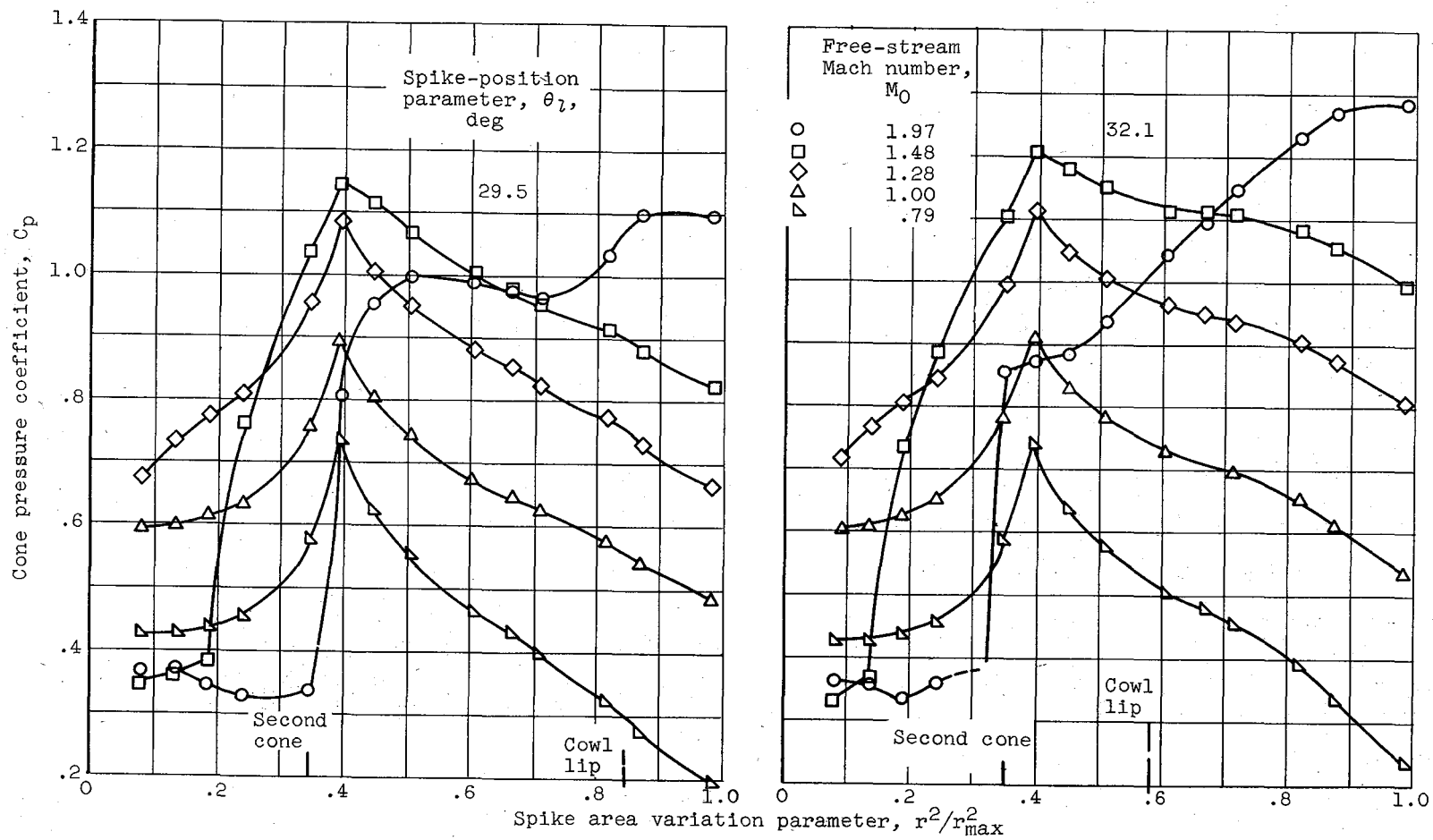


Figure 8. - Typical external cowl pressure distributions near critical mass flows. Spike-position parameter,  $\theta_1$ ,  $29.5^\circ$ .

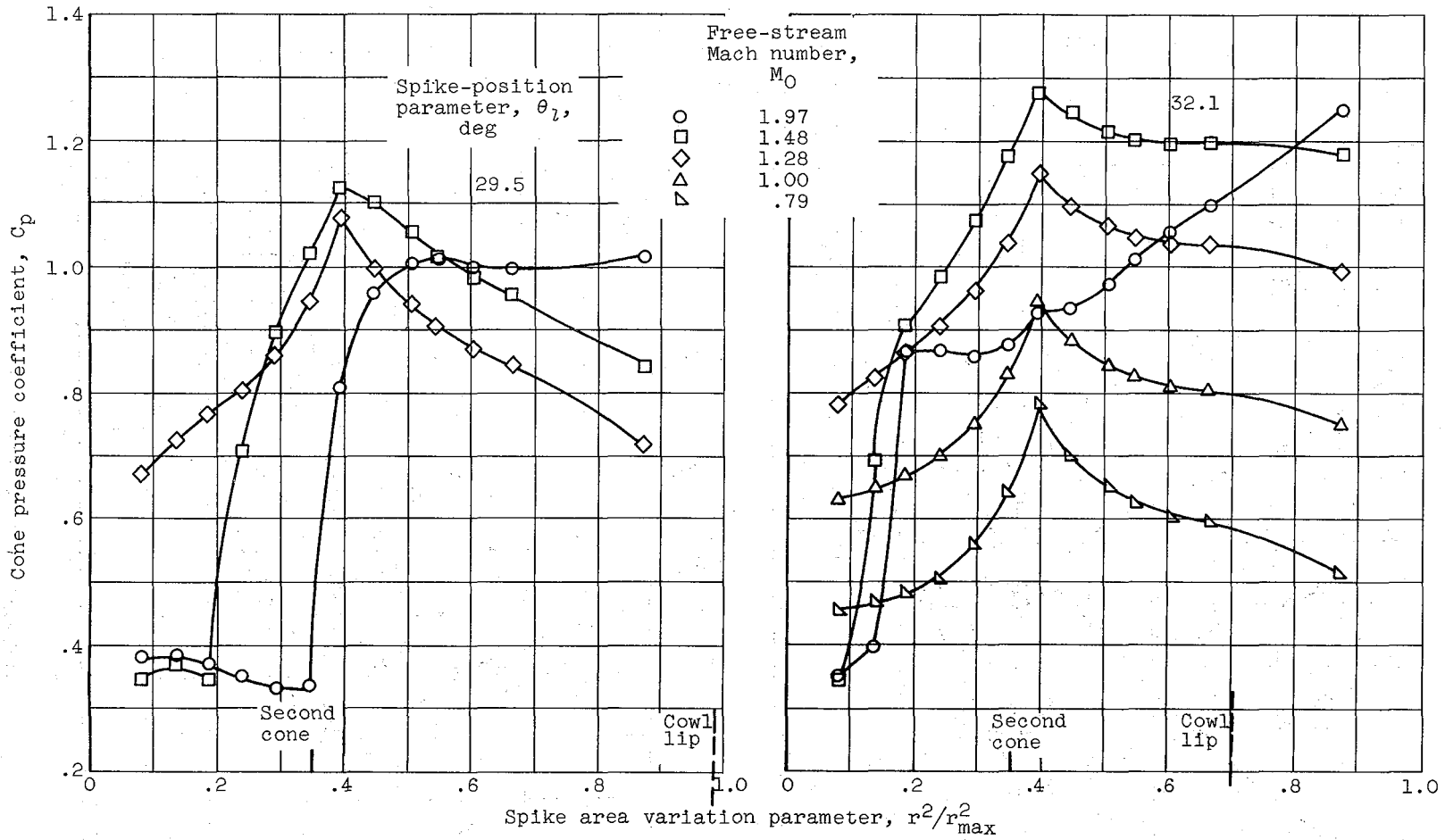
CONFIDENTIAL



(a) 20-Percent cowl.

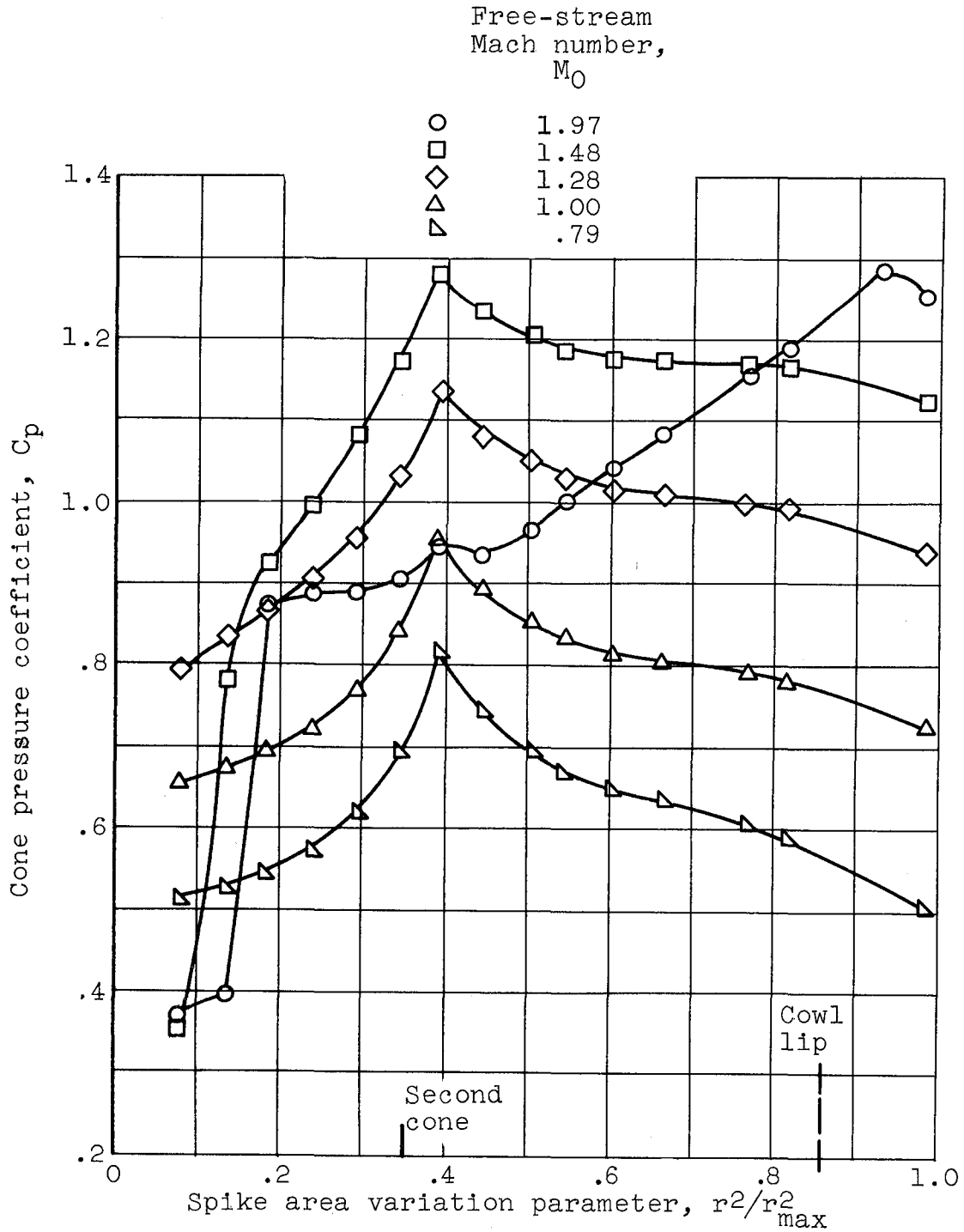
Figure 9. - Typical spike pressure coefficients at critical inlet flow.

CONFIDENTIAL



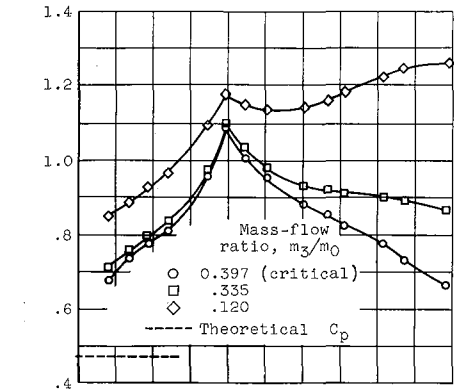
(b) 10-Percent cowl.

Figure 9. - Continued. Typical spike pressure coefficients at critical inlet flow.

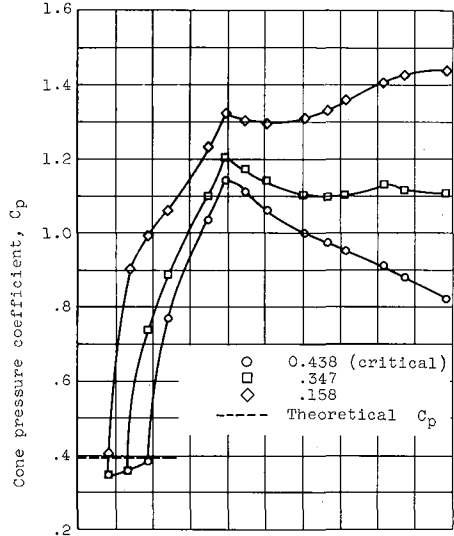


(c) 0-Percent cowl; spike-position parameter,  $\theta_2, 32.1^\circ$ .

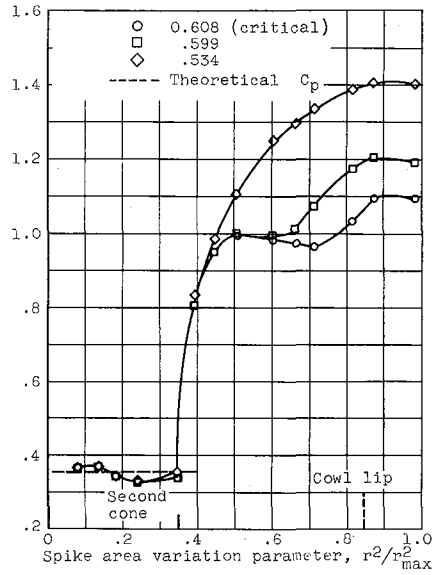
Figure 9. - Concluded. Typical spike pressure coefficients at critical inlet flow.



(a) Free-stream Mach number, 1.28.

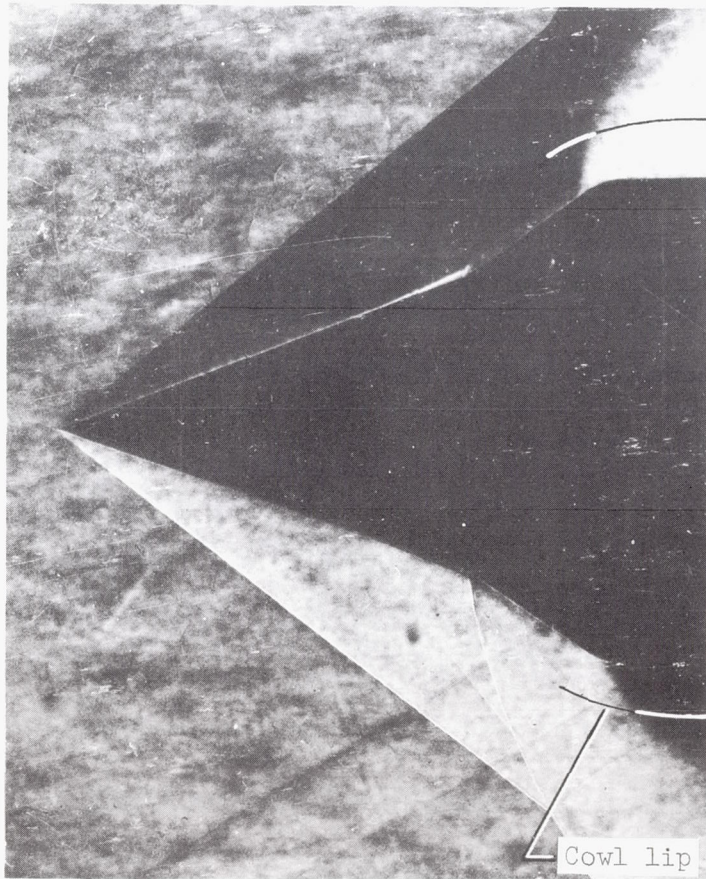


(b) Free-stream Mach number, 1.48.

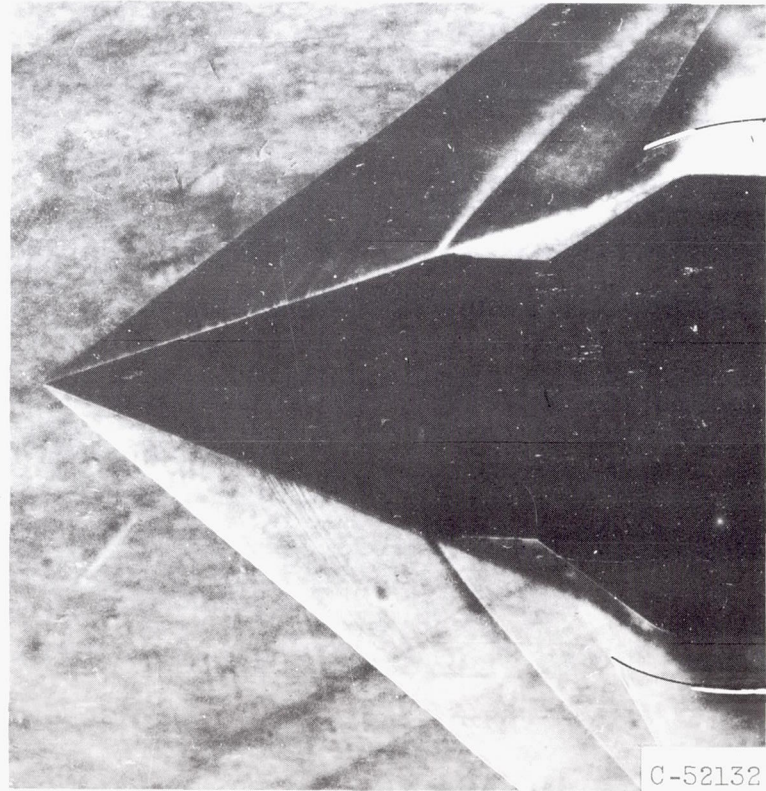


(c) Free-stream Mach number, 1.97.

Figure 10. - Spike pressure coefficients for 20-percent cowl with spike-position parameter,  $\theta_2$ , of  $29.5^\circ$ .



(a)  $20^{\circ}$ - $35^{\circ}$  Spike.



(b)  $20^{\circ}$ -Extended simulated single cone.

Figure 11. - Schlieren photographs at Mach number 1.91 of extended spike.

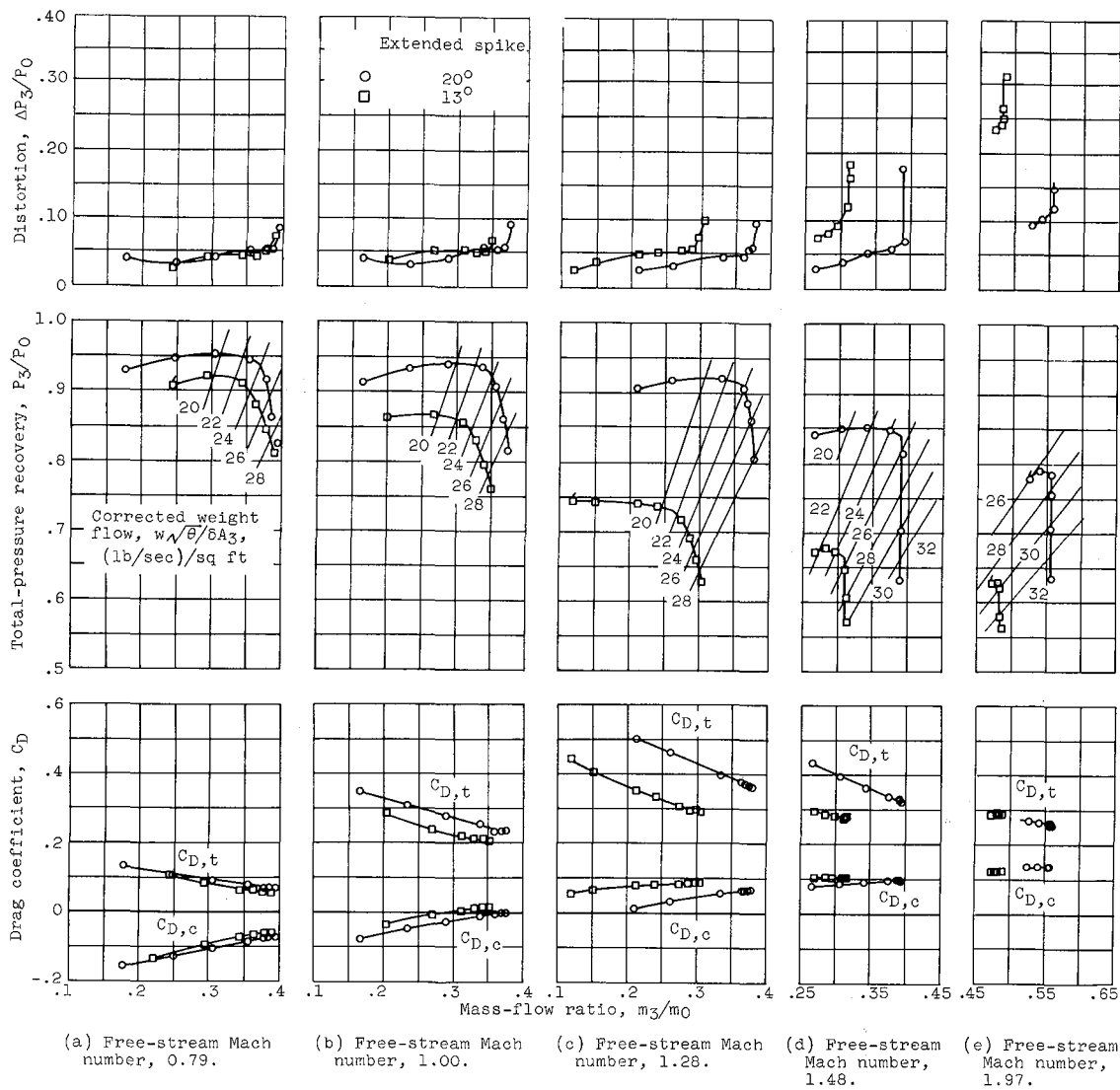


Figure 12. - Performance of extended-spike configurations.

E-151

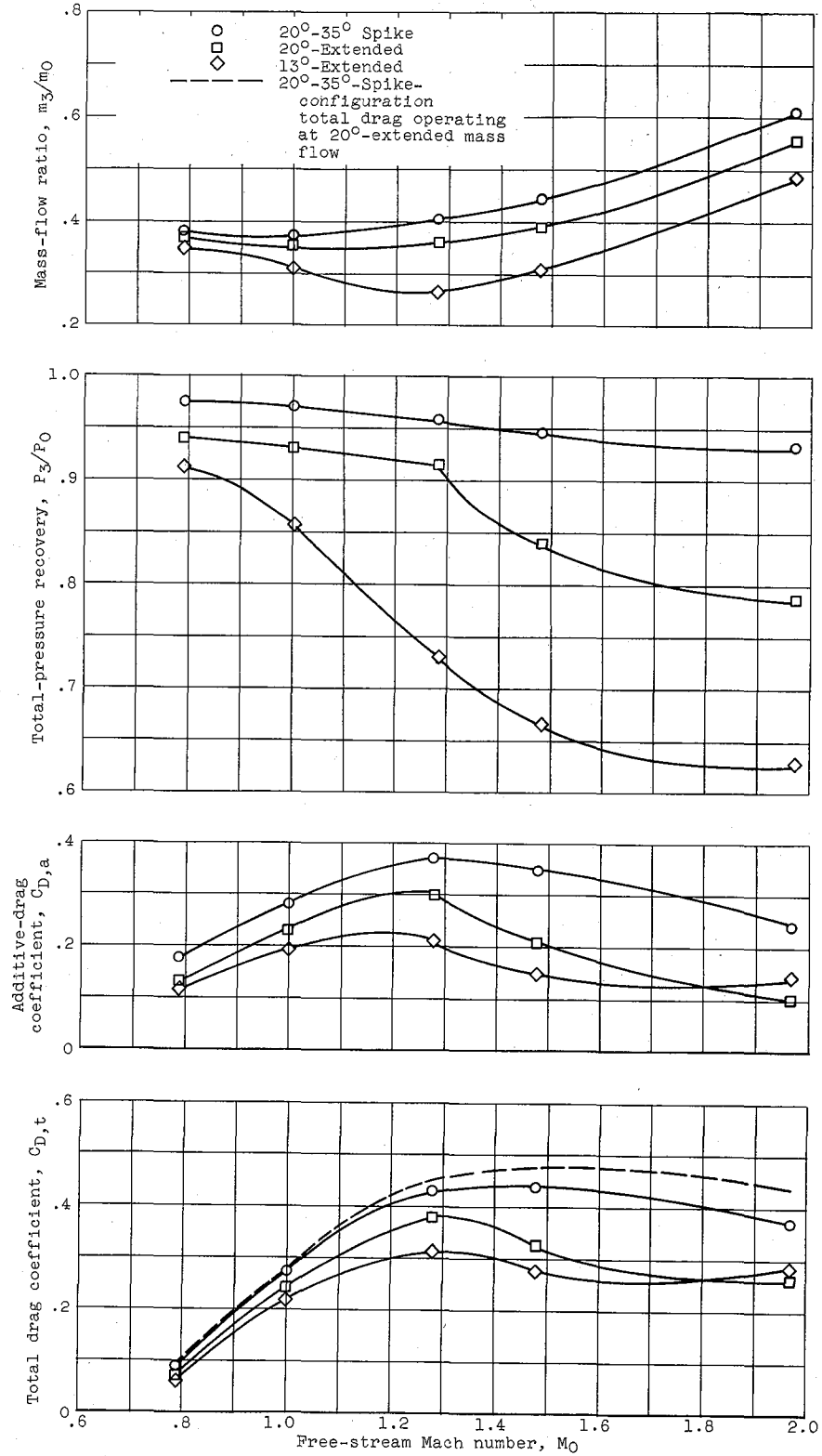


Figure 13. - Performance summary of extended-spike configurations.

DECLASSIFIED

CONFIDENTIAL

CONFIDENTIAL